

# Synthesis, Structural Elucidation, Fire Retardancy and Mechanical Properties of Cyclotriphosphazene Derivatives Blended with Polyurethane Lacquer as Wood Coatings

Nurul Atiqah Mohd Taip<sup>1</sup>, Zuhair Jamain<sup>1\*</sup> and Ismawati Palle<sup>2</sup>

<sup>1</sup>Organic Synthesis and Advanced Materials (OSAM) Research Group, Faculty of Science and Natural Resources, Universiti Malaysia Sabah (UMS), 88400 Kota Kinabalu, Sabah, Malaysia

<sup>2</sup>Faculty of Tropical Forestry, Universiti Malaysia Sabah (UMS), 88400 Kota Kinabalu, Sabah, Malaysia

\*Corresponding author (e-mail: zuhairjamain@ums.edu.my)

This study synthesized cyclotriphosphazene derivatives and evaluated their fire retardancy and mechanical properties for use in wood coatings. Two hexasubstituted cyclotriphosphazene derivatives with dodecyl and hydroxy groups were successfully synthesized. These compounds were subsequently characterized by FTIR and NMR spectroscopy and CHN elemental analysis. The thermal stability of the cyclotriphosphazene compounds was assessed using TGA, while the fire-retardant properties of each coating were evaluated through LOI. Both compounds exhibited good fire retardancy compared to pure epoxy resin, with LOI values of 24.71 (dodecyl) and 25.80 (hydroxy) wt.%, respectively. The LOI results show that coatings made with these nitrogen- and phosphorus-containing compounds demonstrated a significantly improved retardant effect when combined with polyurethane lacquer, compared to polyurethane alone. In addition, the physical and mechanical properties of these derivatives were analysed to assess potential drawbacks of the additives. The essential indicators of the quality of the lacquered wood panel surfaces were: the determination of resistance to household chemicals (ASTM D 1308-2), determination of temperature change resistance (ASTM D1211-97 (2001)), determination of adhesion: cross-cut test (ISO 2409-2007(E)), determination of impact (BS 3962 Part 6:1980) and determination of abrasion (ASTM 4060-10). These tests revealed that the performance of the surface coating systems was significantly influenced by the coating formulation.

**Keywords:** Fire retardant; cyclotriphosphazene; polyurethane lacquer; wood coating

*Received: November 2024; Accepted: January 2025*

Due to the widespread use of wood in decorative items, furniture and architectural applications, as well as various other products, many clear lacquers affect the natural colour of wood during application. This often gives the wood a darker yellow or reddish hue [1, 2]. Despite efforts over the years to develop effective clear coatings for wood, no options currently match the durability and performance of opaque coatings. However, recent studies have shown promising developments, suggesting that clear coatings can potentially surpass the two-year durability benchmark common among commercial products [3].

Wood coatings are primarily applied for two purposes: to protect the wood surface during product use and to achieve a desired visual appearance [4]. The performance of the surface system depends on the quality and type of coating, as well as the compatibility between the wood substrate and coating material. The final quality of the coating is also heavily influenced by the finishing process, including both application and curing stages. When these factors align, the coating system effectively protects wood

flooring against various stresses and potential damage. Essential properties for interior wood flooring include deformability, impact resistance, resistance to liquids, friction, scratching, and abrasion - all of which are measurable by international standards [5].

Polyurethane coatings are well-regarded for their excellent adhesion and abrasion resistance, particularly when compared to materials like rubber, plastic, and metal. However, their adhesion and abrasion resistance can be further enhanced by the addition of specific additives [6]. El-Wahab *et al.* (2020) found that the adhesion properties of polyurethane coatings were not adversely affected when a prepared ligand and its Cu complex were added as additives [7]. Another drawback of polyurethane is its low thermal resistance. According to Ding *et al.* (2021), pure polyurethane had an LOI value of only 19 %, making it extremely flammable [8]. This particular drawback may be improved by the addition of fire retardant additives. Generally, these additives are incorporated into combustible products to delay ignition, suppress flames, and reduce the rate at which fire spreads when exposed to direct flame [9].

The use of halogenated fire retardants in commercial applications has been restricted due to their release of toxic gases during the curing process, which poses environmental concerns. Consequently, there is a growing need for fire retardant compounds that offer high fire resistance while minimizing environmental contamination [1,11]. In the past, bromine-containing fire retardants such as (Tetrabromobisphenol-A (TBBPA) and Tetrabromophthalic anhydride (TBPA) were used as fire retardants, but due to the corrosive effect of HBr emitted during combustion and toxicity of their combustion products, they have been replaced by other alternatives [12]. Fire retardants containing phosphorus and nitrogen have recently emerged as the most promising alternatives to halogen-based options. However, meeting fire safety standards often requires high loading levels, which can significantly reduce the material's strength and other properties. Therefore, developing high-efficiency fire retardants is essential to minimize these negative effects on mechanical performance [13].

One alternative is to use compounds based on hexachlorocyclotriphosphazene (HCCP). HCCP compounds are cyclic structures where the six carbon atoms of a benzene ring are replaced by three nitrogen (N) atoms and three phosphorus (P) atoms. The nitrogen and phosphorus atoms are arranged so that each nitrogen atom is positioned between two phosphorus atoms and vice versa. Surface functionalization of HCCP is easily achieved by replacing the two chlorine atoms attached to phosphorus with various nucleophiles, such as water, amines, or alcohols [14-16]. Ma *et al.* (2019) reported the synthesis of intumescent transparent coatings based on HCCP, incorporating allyl-functionalized phosphonitrile (HABP), trimethylolpropane tris(3-mercaptopropionate) (TMMP), and 1H,1H,2H,2H-perfluorodecanethiol (PFDT). These coatings were produced through photoinduced thiol-ene reactions without the need for a photoinitiator. This compound was then fabricated and applied to the wood coating. Results indicated that incorporation of these HCCP based compounds in the wood coating did not influence the abrasive resistance of the coating, which still showed good anti-abrasion properties [17]. Huang *et al.* (2019) successfully synthesized the novel polybasic carboxylic acid HCPVC consisting of vanillin and HCCP by a nucleophilic substitution reaction and Pinnick oxidation, and then added it to epoxy resin. Results showed that the HCPVC-EP wood coatings exhibited excellent cross-cut adhesion [18].

Next, the fire retardant properties of these compounds were assessed using the limiting oxygen index method (LOI). This is a test used to assess the fire retardancy properties of the additives. The LOI refers to the minimum oxygen concentration (as a percentage) necessary to sustain combustion in a polymer. It is measured by passing a mixture of oxygen and nitrogen over a burning specimen, while

gradually reducing the oxygen level until it reaches the critical threshold. A higher required oxygen concentration indicates greater fire retardancy in the sample [19]. Since atmospheric air contains about 21 % oxygen, a material with an LOI below 21 % would easily burn in air, while an LOI between 21 % and 28 % would classify the material as "slow-burning". Materials that stop burning once the ignition source is removed are considered self-extinguishing [7]. Literature studies by Cao *et al.* (2017) found that the LOI value of acrylonitrile-butadiene-styrene copolymer (ABS) could reach as high as 25.6 % when hexakis(4-nitrophenoxy) cyclotriphosphazene (HNTP) was incorporated into it, which thus improved the intumescent flammability of ABS [20].

In this work, novel cyclotriphosphazene compounds were synthesized via nucleophilic substitution and then blended with commercial polyurethane lacquer as additives, to create a coating film with excellent fire retardant and mechanical properties. Several tests were conducted to evaluate the functionality of the coating film. The LOI test was performed to assess the fire retardant properties of the additives, while thermogravimetric analysis (TGA) was used to analyse the thermal degradation of each additive. The physical and mechanical properties of the coating film were assessed according to ASTM D1308-2, ASTM D1211-97 (2001), BS 3962 Part 6:1980, and ASTM 4060-10 standards. The objectives of this study were to synthesize these derivatives and determine their effectiveness in improving the fire resistance and mechanical performance of wood coatings.

## EXPERIMENTAL

### Chemicals and Materials

In this study, the chemicals used included 4-aminophenol, *N,N*-dimethylformamide, methanol, 4-hydroxybenzaldehyde, potassium carbonate, potassium iodide, anhydrous *n*-hexane, sodium sulfate, glacial acetic acid, dichloromethane, ethyl acetate, polyurethane lacquer, polyurethane sealer, thinner, and hardener. All solvents and chemicals were sourced from Sigma-Aldrich (Steinheim, Germany), Merck (Darmstadt, Germany), Acros Organic (Geel, Belgium), BDH Laboratory (British Drug Houses, Nichiryo, Japan), Polycure Coating (Selangor, Malaysia), and QREC (Asia) (Selangor, Malaysia), and were used without further purification.

### Characterization Methods

Thin Layer Chromatography (TLC) was employed to identify products in a mixture and to monitor the progress of the reaction. A 1:1 mixture of ethyl acetate and hexane was prepared as solvent. FTIR spectroscopy (Bruker, UK) was utilized to identify the functional groups present in the synthesized compounds. Compounds were scanned over a range

of 600-4000  $\text{cm}^{-1}$ . The molecular structures of the compounds were determined by NMR spectroscopy with a Bruker 500 MHz Ultrashield™ spectrometer (Bruker, Coventry, UK), targeting atomic nuclei such as  $^1\text{H}$ ,  $^{13}\text{C}$ , and  $^{31}\text{P}$ . The percentages of carbon, hydrogen, and nitrogen in each compound were measured using CHN elemental analysis (CHN analyzer, model PerkinElmer II, 2400, Waltham, MA, USA) by burning the sample in excess oxygen. The precision and accuracy of the CHN analyzer results are significantly affected by the purity of the substances being examined. Poor sample preparation may leave moisture residues, solvent contaminants, sampling errors, and changes in composition and heterogeneity in the tested sample. Volatility may also cause these changes. All the aforementioned factors could invalidate the elemental analysis results [21]. Thermogravimetric analysis (TGA) is a method for evaluating a sample's thermal stability. For the HCCP, the TGA was conducted between 50 and 700 °C at 10 °C/min with a constant flow rate of 30 mL/min. A 10 mg sample in an alumina crucible was placed in a thermogravimetric analyser. The LOI test, conducted using equipment from S.S. Instruments Pvt. Ltd. (Delhi, India), was employed to evaluate the fire-retardant properties of the HCCP additives. This test determined the minimum oxygen concentration in a nitrogen mixture that could sustain the combustion of the material under equilibrium conditions resembling candle-like burning [22]. The LOI testing was performed using an FTT oxygen index, adhering to BS 2782: Part 1: Method 141, as well as the standardized tests ISO 4589-1: 2017 and ASTM D: 2863-17a. The wood panel measured 150 mm x 10 mm x 10 mm. The data were expressed as percentages (%), and the LOI results were calculated using the specified formula (Equation 1):

$$\text{LOI} = C_F + (k \times d) \quad (\text{Eq. 1})$$

Where  $C_F$  is the oxygen concentration of the final test,  $k$  is a factor taken from the Fire Testing Technology (ISO 4589) manual and  $d$  is the oxygen concentration increment.

Next, a colour reader was used to obtain colour readings for all the samples before they were exposed to the temperature change resistance test. Six conditions were controlled for visual evaluation: (1) the spectral quality of the light source; (2) the intensity of the light source; (3) the angular size of the light source; (4) the angle from which light strikes the object; (5) the angle at which the object is viewed; and (6) the background colour.

The colour changes in the samples were measured before and after one day of exposure to household chemical tests. Colour measurements were taken using a Konica Minolta Spectrophotometer (CM-2002) based on the CIE  $L^*a^*b^*$  colour system in SCE mode (specular component excluded). The

colour change ( $\Delta E$ ) was then calculated in accordance with ASTM D2244, as detailed in Equation 2.

$$\Delta E = (\Delta L^{*2} + \Delta a^{*2} + \Delta b^{*2})^{1/2} \quad (\text{Eq. 2})$$

$\Delta E$  = Value of colour difference

$L^*$  = Brightness value (The higher the value, colour becomes white (0 % (black) to 100 % (white))

$a^*$  = Colour index (The higher the value, colour becomes more red (green (-a) to red (+a))

$b^*$  = Colour index (The higher the value, colour becomes more yellow (blue (-a) to yellow (+a))

### Physical and Mechanical Testing

This research used plywood for the LOI, physical and mechanical testing. Plywood is a product that has traditionally played an important role in light framework construction and structural materials. It also had been widely used in the manufacture of furniture, housing, and other industrial products.

#### *Resistance to Household Chemicals (ASTM D 1308-2)*

The resistance to household chemicals test is intended to observe the resistance of the wood finishing against domestic chemicals and detergents that may spill onto the wood surface. The test was performed according to ASTM D 1308-2 at a temperature of  $23 \pm 2$  °C with a relative humidity of  $50 \pm 5$  % for a maximum of 24 hours. The dimensions of the wood panel were 300 mm x 95 mm x 10 mm. A small portion of a reagent was placed on the surface of the horizontal wood panel. After a specific time interval, the spot was wiped clean and examined immediately for effects. The wood panel was divided into eight columns evenly and numbered. Different household chemicals were systematically applied on the wood panel for testing. The reagents were chosen based on ultimate coating use. The reagents used in this test were hot and cold distilled water, 50 % ethyl alcohol, alkali solution, acid solution, soap solution and detergent solution. A coffee solution prepared in 100 mL hot distilled water, and a pea-sized amount of ketchup were also applied on the wood surface.

#### *Temperature Change Resistance (ASTM D1211-97 (2001))*

This test was conducted in accordance with ASTM D1211-97 (2001), a method used to assess the resistance of clear lacquer coatings on wood or plywood substrates to checking and cracking when exposed to rapid temperature changes. Clear coatings on wood often fail by forming cracks over time, either along the grain or at an angle. This test accelerates the development of these defects by cycling the temperature.

Wood samples in dimensions of 300 mm x 95 mm x 10 mm were prepared for every parameter.

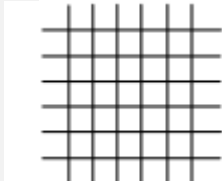
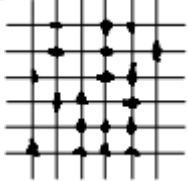
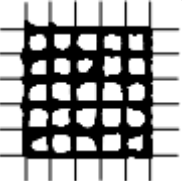
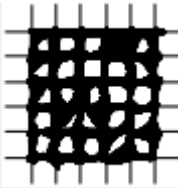
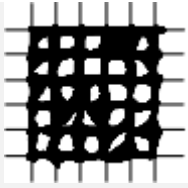
Firstly, the Minolta Colour Reader was used to obtain the colour readings for all the samples before they were exposed to the temperature change resistance test. One wood panel for each parameter was stacked in a conditioning room as the sample exposed to a controlled environment, while nine wood panels were used for testing at hot and cold temperatures. The selected panels were placed in the oven for one hour at  $50 \pm 3$  °C before the being transferred within one minute to a freezer and maintained at  $10 \pm 2$  °C for another hour. The wood panels were then removed from the freezer and left at room temperature for 30 minutes, where 15 minutes were allocated as a relaxation period and another 15 minutes for inspection, to observe a change in colour or any other defects that occurred on the coating surfaces. The change of colour was determined by using the colour reader, and the reading was recorded. The wood panels were first exposed to high temperature, followed by low temperature, and then returned to room temperature within a specified time frame, completing one

cycle. This process was repeated for a total of four cycles.

**Cross-cut Adhesion (ISO 2409-2007(E))**

The test panel was prepared according to the ISO 2409-2007(E) Paint and Varnishes: Cross-cut Test standard, and then coated using the specified method with the final compound. Each coated test panel was dried immediately at a temperature of  $(23 \pm 2)$  °C with a relative humidity of  $(50 \pm 5)$  % for a minimum of 16 hours. The dimensions of this test sample were 300 mm x 95 mm x 10 mm. A cross guide knife was used to make cuts at a depth of 0.2 mm on the coating surface. A lattice with six cuts spaced at 1 mm in each direction was made on the coating film. To obtain an average rating, three areas were used for the cross-cut test in one sample. The cut area was then brushed gently to clear the surface before being observed with a hand lens. The cut appearance and degree of finish removed were assessed on a scale of 1 to 5, according to the ISO 2409-2007 standard (Table 1).

**Table 1.** Classification of adhesion according to the Cross-cut test [23].

Rating	Rating 0	Rating 1	Rating 2
Surface of Cross-cut area from which flaking has occurred	None	<5%	5-15 %
			
	Rating 3	Rating 4	Rating 5
	15-35 %	35-65 %	>65 %
			-

**Table 2.** Impact test rating code description according to BS 3962 Part 6: 1980.

Classification	Description
5	No surface cracking
4	Slight cracking e.g.: one or two circular cracks around the edge of indentation
3	Moderate or severe cracking confined to the area of indentation
2	Cracking extending outside the area of indentation and/or slight flaking of the finish
1	More than 25 % of the finish removed from the area of indentation

### Impact (BS 3962 Part 6:1980)

The resistance of a wood finish to impact can be determined using a ball drop impact test, according to BS 3962 Part 6: 1980 Resistance to Mechanical Damage Impact, with the sample size of 300 mm x 95 mm x 10 mm. This was done by dropping a 43 mm diameter steel ball with a weight of 393 g on the finishing surface from a 1 m height. The test area was then inspected with a hand lens, and the degree of finish cracking was rated on a scale of 1 to 5, following the BS 3692 Part 6: 1980 standard (Table 2).

### Abrasion Testing (ASTM 4060-10)

Abrasion of the surface occurs when there is friction between two surfaces, which causes the surface to peel off. The abrasion resistance test was conducted using a rotating abrasive wheel (loaded with 1000 g) at a speed of 100 cycles per minute on a sample measuring 100 x 100 x 10 mm<sup>3</sup>, in accordance with ASTM 4060-10 for abrasion resistance of organic coatings by the Taber Abraser. The samples were weighed before and after the completion of every 100 cycles. The abrasion resistance was calculated based on Equation 3 below.

$$L = A - B \quad (\text{Eq. 3})$$

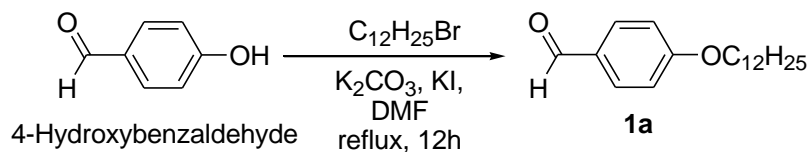
where A is the weight of the test specimen before abrasion in mg, and B is the weight of the test specimen after abrasion, in mg.

### Synthesis Methods

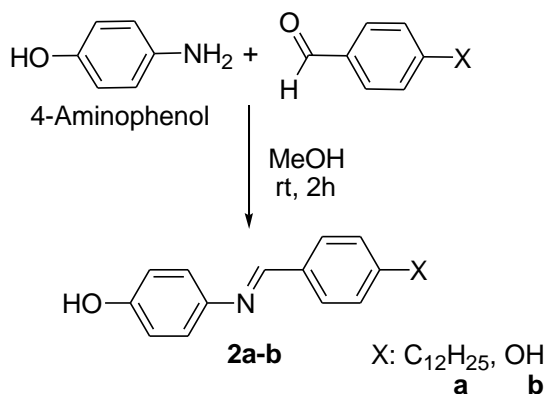
Intermediate **1a** was synthesized through the alkylation reaction of 4-hydroxybenzaldehyde with dodecyl bromide, as shown in Scheme 1 [24]. The reaction of 4-aminophenol with 4-substituted benzaldehydes in methanol produced intermediates **2a-b**, depicted in Scheme 2 [25,26]. Finally, the reaction between HCCP (N<sub>3</sub>P<sub>3</sub>Cl<sub>6</sub>) and intermediates **2a-b** yielded the final compounds **3a-b**, as illustrated in Scheme 3 [27,28]. The percentage yields of the synthesized compounds were calculated using Equation 4.

$$\text{Percent yield} = \frac{\text{Actual yield}}{\text{Theoretical yield}} \times 100 \% \quad (\text{Eq. 4})$$

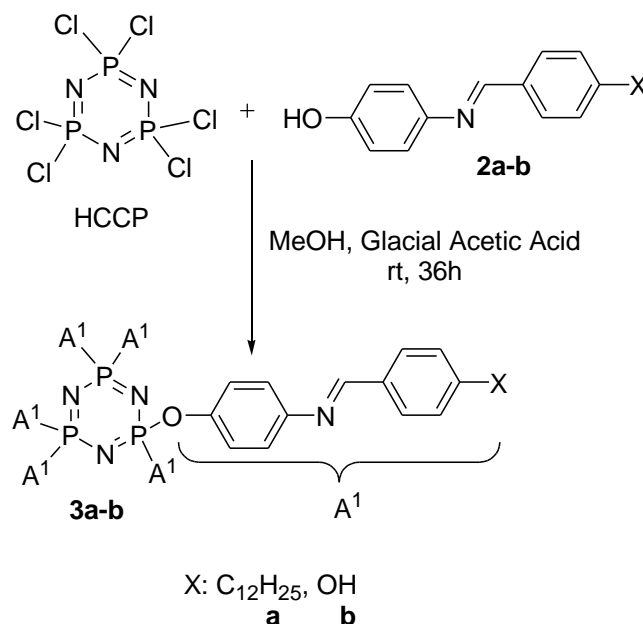
In this study, FTIR and NMR spectroscopy, and CHN elemental analysis were used to characterize the synthesized compounds. To prepare the sample, 1 g of compound **3a** was first diluted in methanol and then mixed into 100 mL of polyurethane lacquer. Thinner and hardener were subsequently added in a 1:5:5 ratio of polyurethane lacquer, thinner, and hardener. The wood panels were checked to ensure they were free of any surface contaminants or imperfections. The mixture was then stirred homogeneously before being applied to the wood panel using a brush. The final dry film had a thickness of around 90-100 μm. To remove any remaining solvent, the wood panels were air-dried for 10 days and then placed in an oven at 50-60 °C for two hours before undergoing LOI testing to investigate their fire-retardant properties [29].



**Scheme 1.** Alkylation reaction of intermediate **1a**.



**Scheme 2.** Condensation reaction of intermediates **2a-b**.



**Scheme 3.** Formation of compounds **3a-b**.

## Syntheses

### Synthesis of 4-dodecyloxybenzaldehyde, **1a**

4-Hydroxybenzaldehyde (0.1 mol) and 1-bromododecane (0.1 mol) were dissolved separately in 20 mL of *N,N*-dimethylformamide. The two solutions were then mixed in a 250 mL round-bottom flask. Potassium carbonate (0.15 mol) and potassium iodide (0.01 mol) were added to the mixture, which was refluxed for 12 hours. The progress of the reaction was monitored using TLC. After completion, the mixture was poured into 500 mL of cold water and extracted with dichloromethane. The organic layers were collected, dried over anhydrous sodium sulfate, filtered, and evaporated overnight. Yield: 24.94 g (85.86 %), light yellow oil. FTIR (cm<sup>-1</sup>): 2922 and 2852 (asymmetrical and symmetrical Csp<sup>3</sup>-H stretching), 2732 ( $\underline{\text{H-CO}}$ , aldehydic stretching), 1688 (C=O stretching), 1599 (C=C stretching), 1254 (C-O stretching). <sup>1</sup>H NMR (500 MHz, CDCl<sub>3</sub>)  $\delta$ , ppm: 9.76 (s, 1H), 7.72 (d, *J*=4.8, 2H), 6.82 (d, *J*=8.94, 2H), 3.93 (t, *J*=6.18, 2H), 1.70-1.72 (m, 2H), 1.17-1.38 (m, 2H), 0.80 (t, *J*=6.90, 3H). <sup>13</sup>C NMR (125 MHz, CDCl<sub>3</sub>)  $\delta$ , ppm: 190.2, 164.1, 131.7, 129.6, 114.5, 68.5, 31.1, 29.6, 29.5, 25.9, 14.0.

### Synthesis of (*E*)-4-((4-dodecylbenzylidene)amino)phenol, **2a**

A solution containing 4-aminophenol (0.02 mol) and 4-dodecyloxybenzaldehyde (0.02 mol) in 40 mL of methanol were mixed in a round-bottom flask. The mixture was stirred for about 2 hours at room temperature, and TLC was used to monitor the progress of the reaction. It was then transferred into

250 mL of cold water, filtered, and allowed to dry for several days. The same method was applied to synthesize intermediate **2b**. Yield: 5.81 g (76.18 %), light brown powder. FTIR (cm<sup>-1</sup>): 3064 (O-H stretching), 2955 and 2849 (symmetrical and asymmetrical Csp<sup>3</sup>-H stretching), 1605 (C=N stretching), 1573 (C=C stretching), 1288 (C-O stretching). <sup>1</sup>H NMR (500 MHz, DMSO-*d*<sub>6</sub>)  $\delta$ , ppm: 8.48 (s, 1H), 7.81 (d, *J*=10 Hz, 2H), 7.14 (d, *J*=10 Hz, 2H), 7.00 (t, *J*=10 Hz, 2H), 6.78 (d, *J*=5 Hz, 2H), 4.00 (m, 2H), 1.72 (m, 2H), 1.41-1.21 (m, 2H), 0.84 (t, 3H). <sup>13</sup>C NMR (125 MHz, DMSO-*d*<sub>6</sub>)  $\delta$ , ppm: 161.39, 157.17, 156.27, 143.44, 130.45, 129.61, 122.70, 116.14, 115.10, 68.14, 40.45, 40.35, 40.28, 40.18, 40.02, 39.85, 39.68, 39.52, 39.53, 31.73, 29.45, 29.44, 29.41, 29.39, 29.16, 29.14, 29.01, 25.89, 22.53, 14.40. CHN Elemental Analysis: Calculated for C<sub>25</sub>H<sub>35</sub>NO<sub>2</sub> C: 78.70% H: 9.25% N: 3.67% Found: C: 78.61% H: 9.21% N: 3.57%.

### Synthesis of (*E*)-4-((4-hydroxybenzylidene)amino)phenol, **2b**

Yield: 4.16 g (97.55 %), light brown powder. FTIR (cm<sup>-1</sup>): 3100 (O-H stretching), 1639 (C=N stretching), 1577 (C=C stretching), 1235 (C-O stretching). <sup>1</sup>H NMR (500 MHz, DMSO-*d*<sub>6</sub>)  $\delta$ , ppm: 8.69 (s, 1H), 8.04 (d, *J*=10 Hz, 2H), 8.00 (d, *J*=10 Hz, 2H), 7.26 (t, *J*=5 Hz, 2H), 6.82 (d, *J*=5 Hz, 2H). <sup>13</sup>C NMR (125 MHz, DMSO-*d*<sub>6</sub>)  $\delta$ , ppm: 167.47, 157.19, 156.56, 142.58, 140.59, 132.87, 130.15, 128.70, 123.27, 116.27, 40.32, 40.25, 40.15, 39.99, 39.82, 39.65, 39.49, 39.32. CHN Elemental Analysis: Calculated for C<sub>13</sub>H<sub>11</sub>NO<sub>2</sub> C: 73.23% H: 5.20% N: 6.57% Found: C: 73.01% H: 5.11% N: 6.48%.

***Synthesis of Hexakis(oxy-4-[(4-dodecyloxy-benzylidene)-  
-amino] triazophosphazene, 3a***

Hexachlorocyclotriphosphazene ( $N_3P_3Cl_6$ ) (0.01 mol) was reacted with intermediate **2a** in 40 mL of methanol. Two drops of glacial acetic acid were added as a catalyst. The mixture was stirred for approximately 36 hours at room temperature, with TLC used to monitor the progress of the reaction. Afterwards, the mixture was transferred into 250 mL of cold water, filtered, and allowed to dry for several days. The same procedure was applied to synthesize intermediate **3b**. Yield: 2.08 g (85.97 %). Light green powder. FTIR ( $cm^{-1}$ ): 2916 and 2849 (Csp<sup>3</sup>-H stretching), 1601 (C=N stretching), 1507 (C=C stretching), 1249 (C-O stretching), 1159 (P=N stretching), 971 (P-O-C bending). <sup>1</sup>H NMR (500 MHz, DMSO-d<sub>6</sub>)  $\delta$ , ppm: 8.46 (d, 2H), 7.95 (d, *J*=5 Hz, 2H), 7.50 (d, *J*=10 Hz, 2H), 7.12 (d, *J*=5 Hz, 2H), 6.82 (d, *J*=10 Hz, 2H), 4.04 (t, *J*=5 Hz, 2H), 1.26-1.76 (m, 2H), 0.87 (t, *J*=5 Hz, 3H). <sup>13</sup>C NMR (125 MHz, DMSO-d<sub>6</sub>)  $\delta$ , ppm: 161.61, 156.75, 156.35, 143.94, 138.25, 132.00, 128.94, 122.37, 116.31, 68.56, 40.92, 40.75, 40.58, 40.41, 40.25, 40.08, 39.91, 31.65, 29.37, 29.34, 29.31, 29.15, 29.10, 29.07, 29.00, 25.89, 22.35, 14.01. <sup>31</sup>P NMR (500 MHz, DMSO-d<sub>6</sub>)  $\delta$ , ppm: 11.15 (s, 3P). CHN Elemental Analysis: Calculated for C<sub>150</sub>H<sub>204</sub>N<sub>9</sub>O<sub>12</sub>P<sub>3</sub> C: 74.50% H: 8.50% N: 5.21% Found: C: 74.39% H: 8.42% N: 5.14%.

***Synthesis of Hexakis(oxy-4-[(4-hydroxyl-benzylidene)-  
-amino] triazophosphazene, 3b***

Yield: 0.75 g (53.26 %). Dark green powder. FTIR ( $cm^{-1}$ ): 3205 (O-H stretching), 1596 (C=N stretching), 1511 (C=C stretching), 1208 (C-O stretching), 1155 (P=N stretching), 976 (P-O-C bending). <sup>1</sup>H NMR (500 MHz, DMSO-d<sub>6</sub>)  $\delta$ , ppm: 8.54 (s, 1H), 8.08 (d, *J*=10 Hz, 2H), 7.46 (d, *J*=10 Hz, 2H), 7.13 (d, *J*=5 Hz, 2H), 6.69 (d, *J*=10 Hz, 2H). <sup>13</sup>C NMR (125 MHz, DMSO-d<sub>6</sub>)  $\delta$ , ppm: 164.32, 153.55, 148.12, 140.80, 136.43, 129.87, 126.23, 122.75, 116.31, 41.03, 40.85, 40.69, 40.52, 40.35, 40.19, 40.02. <sup>1</sup>H NMR (500 MHz, DMSO-d<sub>6</sub>)  $\delta$ , ppm: 11.20 (s, 3P). CHN Elemental Analysis: Calculated for C<sub>78</sub>H<sub>60</sub>N<sub>9</sub>O<sub>12</sub>P<sub>3</sub> C: 66.52% H: 4.29% N: 8.95% Found: C: 66.48% H: 4.26% N: 8.91%.

## RESULTS AND DISCUSSION

### FTIR Analysis

The FTIR spectrum for intermediate **1a** displayed absorption bands at 2922 and 2852  $cm^{-1}$ , corresponding to symmetrical and asymmetrical Csp<sup>3</sup>-H stretching. The band at 2732  $cm^{-1}$  was attributed to the aldehydic H-CO stretching, while the bands at 1688 and 1599  $cm^{-1}$  were associated with C=O and C=C stretching, respectively. Additionally, C-O stretching was observed at 1254  $cm^{-1}$ . The absence of a broad absorption band for O-H stretching at 3300  $cm^{-1}$  indicated that the insertion of the alkyl group into the benzaldehyde was successful.

The condensation reaction of 4-aminophenol with 4-substitutedbenzaldehyde in methanol produced the intermediate (E)-4-((4-substitutedbenzylidene) amino)phenol, **2a-b**, as shown in Scheme 2, which contained Schiff base linkages. The azomethine group (C=N) for intermediates **2a** and **2b** appeared at 1605 and 1639  $cm^{-1}$ , respectively. Moreover, the FTIR data displayed a characteristic absorption band at ~ 3100  $cm^{-1}$ , corresponding to the stretching vibrations of the alcohol (O-H stretching). The peak associated with C-H stretching was also observed. Additionally, the bands at 2955 and 2849  $cm^{-1}$  were attributed to the symmetrical and asymmetrical Csp<sup>3</sup>-H stretching, respectively. The band at 1573  $cm^{-1}$  corresponded to C=C stretching, while the band at ~ 1250  $cm^{-1}$  was due to C-O stretching. The absence of a band for aldehydic C-H stretching in intermediates **2a** and **2b** further confirmed the success of the condensation reaction.

Intermediate **2a** reacted with HCCP to yield the final compound **3a**, which contained Schiff base linkages, as illustrated in Scheme 3. In the FTIR spectrum of compound **3a** (Figure 1), aromatic C=C and C-O stretching was indicated by absorption bands of 1507 and 1249  $cm^{-1}$ , respectively. P-O-C bending appeared at 971  $cm^{-1}$ , while the absorption band for P=N stretching was detected at 1159  $cm^{-1}$ . An azomethine linkage (C=N) was observed at 1601  $cm^{-1}$ , and symmetrical and asymmetrical Csp<sup>3</sup>-H stretching was seen at 2916 and 2849  $cm^{-1}$ , respectively.

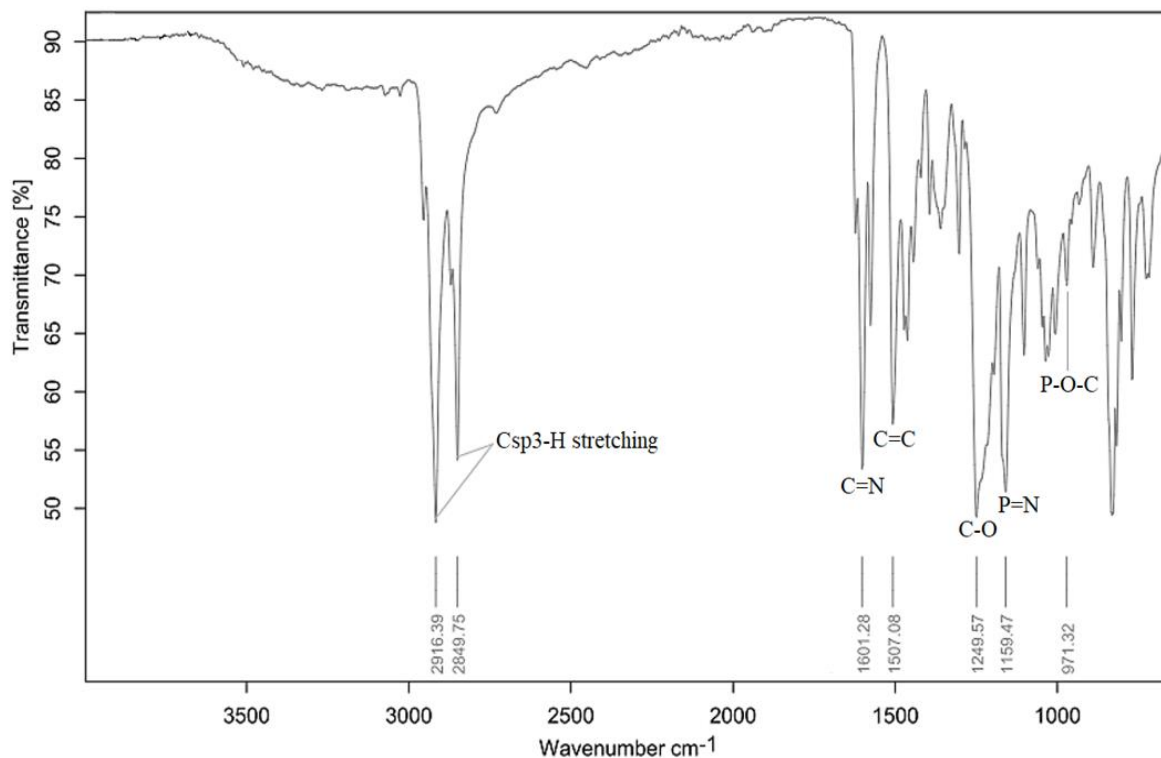


**Figure 1.** Fourier Transform Infrared (FTIR) spectrum of compound **3a**.

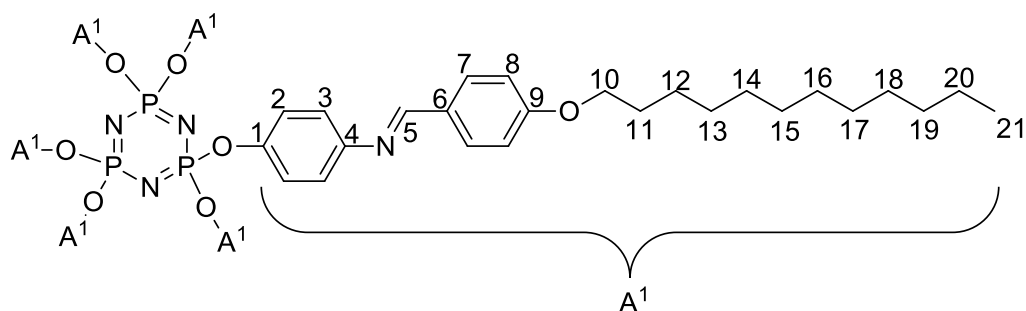


**Figure 2.** Structure of compound **3a** with complete atomic numbering.

### NMR Analysis

In this study, compound **3a** was selected as a representative example, and Figure 2 illustrates the confirmation of its chemical structure, complete with atomic numbering.

The <sup>1</sup>H NMR spectrum of compound **3a** (Figure 3) revealed a prominent signal for the Schiff

base proton, H5, located far downfield at δ 8.46 ppm. In addition, the spectrum displayed four distinct doublets corresponding to different aromatic protons within the compound. These doublets appeared at δ 7.50, 7.12, 7.95, and 6.82 ppm and were assigned to protons H3, H2, H7, and H8, respectively. The specific splitting patterns and chemical shifts observed in the spectrum provide valuable insight into the electronic environments of these protons.

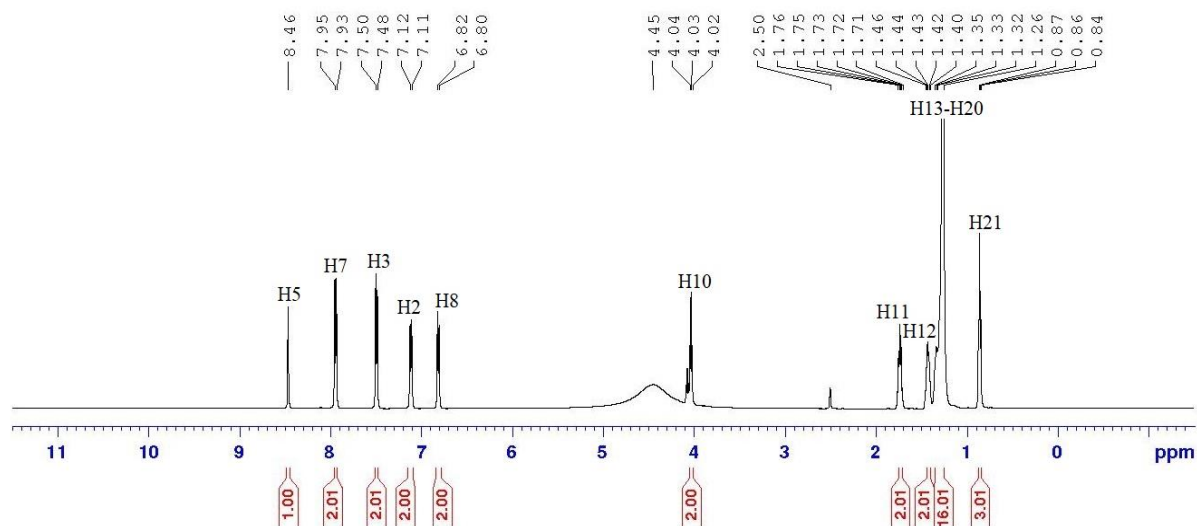


Figure 3.  $^1\text{H}$  NMR (500 MHz,  $\text{DMSO-d}_6$ ) spectrum of compound **3a**.

The  $^{13}\text{C}$  NMR spectrum (Figure 4) of compound **3a** exhibited one Schiff base carbon signal, four quaternary carbon signals, and four aromatic carbon signals. The signal of the Schiff base carbon was at  $\delta$  161.61 ppm (**C5**), while the quaternary carbon resonated at **C1** ( $\delta$  156.35 ppm), **C4** ( $\delta$  143.94 ppm), **C6** ( $\delta$  138.25 ppm) and **C9** ( $\delta$  156.75 ppm). The **C1** peak was further downfield due to the high electronegativity of the cyclotriphosphazene system. As **C4** was attached directly to a nitrogen atom, its signal was further downfield compared to **C6** and **C9**. The aromatic carbon signals were assigned to  $\delta$  132.00

(**C7**), 128.94 (**C3**), 116.31 (**C2**), and 122.37 (**C8**). The same experience as quaternary was responsible for the different chemical experiences.

The  $^{31}\text{P}$  NMR spectrum of compound **3a** (Figure 5) displayed a singlet at  $\delta$  11.15 ppm. This characteristic signal suggests that all phosphorus atoms within the compound were uniformly substituted in the side arms. The presence of a single peak indicates a symmetrical environment around all the phosphorus atoms, implying that there was no difference in their chemical surroundings.

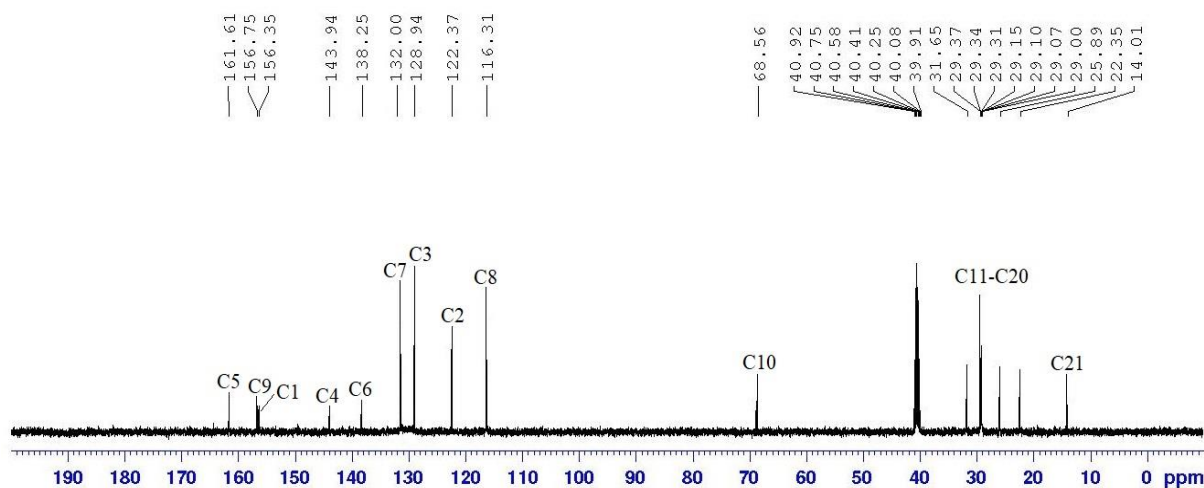


Figure 4.  $^{13}\text{C}$  NMR (125 MHz,  $\text{DMSO-d}_6$ ) spectrum of compound **3a**.

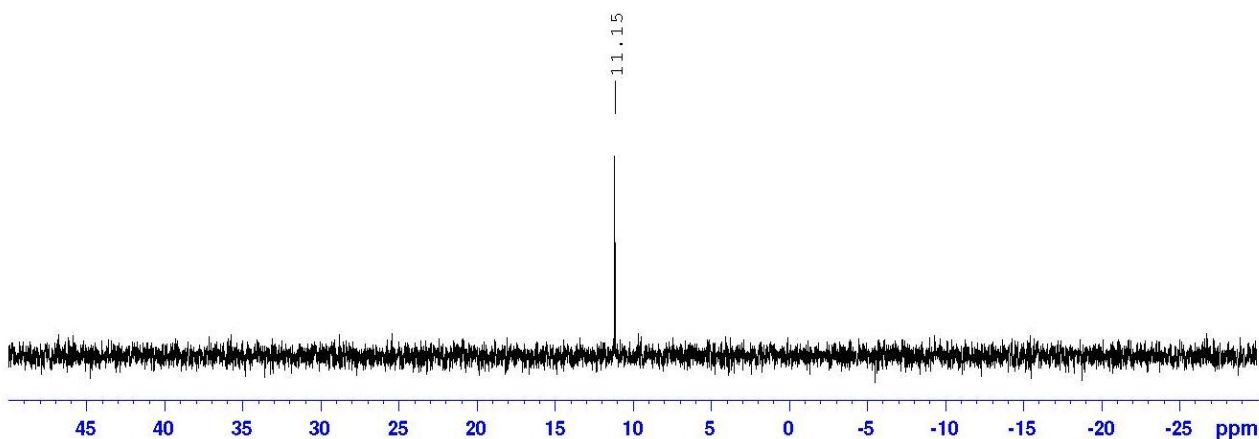


Figure 5.  $^{31}\text{P}$  NMR (500 MHz,  $\text{DMSO-d}_6$ ) spectrum of compound **3a**

### Structure-Property Relationships

In this study, the conjugation of the Schiff base ( $-\text{C}=\text{N}-$ ) linking unit with the phenylene ring resulted in an increase in the molecule's length. This elongation enhanced the anisotropic polarizability and flexibility of the compounds, which in turn limited their rotational freedom [30,31]. Thus, the rigidity and linearity of its constituents were maintained to provide high stability. Compounds with linking units are easier to synthesize compared to compounds with direct bonds because the linking unit provides a point of link up in the synthesis [32].

### Determination of Thermal Properties of HCCP-Based Compounds

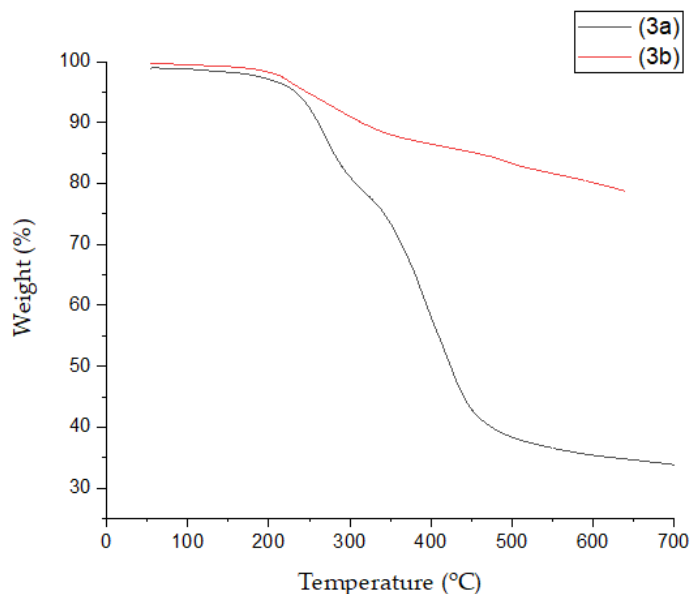
Cyclotriphosphazene, composed of alternating phosphorus and nitrogen atoms, displays exceptional thermal stability [33]. The thermal decomposition and the final char yield of the HCCP-based compounds were studied via TGA analysis and summarized in

Table 3. Figure 6 illustrates the TGA curves of compounds **3a** and **3b** obtained under a nitrogen flow rate of 30 mL/min. The plotted TGA curves showed good thermal stability, with compound **3a** displaying two distinctive weight loss stages while compound **3b** displayed only one distinctive weight loss stage. The final char yields at 700 °C for both compounds **3a** and **3b** were 34.32 % and 78.69 %, respectively.

Overall, both HCCP compounds demonstrated excellent thermal stability, primarily due to the presence of chemically stable P–N skeletons and cross-linking structures [34]. The relatively lower degradation temperature of the HCCP compounds may be attributed to the more readily decomposable P–O–C linkage, which aids in the formation of a char layer that protects the wood matrix [35]. Additionally, this thermal stability may be linked to the ability of Schiff bases derived from p-hydroxybenzaldehyde to form intramolecular hydrogen bonds with the azomethine group, further enhancing the thermal resilience of the HCCP compounds [36,37].

Table 3. Thermal analysis of HCCP compounds.

Compound	Temperature of 5% Weight Loss (°C)	Temperature of most rapid weight loss, $T_{\text{max}}$ (°C)	Char Residue at 700 °C (%)
<b>3a</b>	250	393	34.32
<b>3b</b>	248	375	78.69



**Figure 6.** TGA curves of compounds **3a** and **3b** from 50 to 700 °C at a heating rate of 10 °C/min under a N<sub>2</sub> flow of 30 mL/min.

#### ***Determination of Fire-Retardant Properties of HCCP/PU Compounds***

HCCP compounds were incorporated as additives into the polyurethane lacquer coating. The LOI test was conducted to assess the fire-retardant properties of the HCCP compounds, with polyurethane serving as the coating matrix. Polyurethane was selected for its desirable qualities, including excellent flexibility, low viscosity, fast setting speeds, and good thermal stability [38]. However, the high flammability of polyurethane materials limits their use in everyday applications [39]. In this experiment, only 1 wt.% of each additive was utilized in the sample preparation to achieve maximum fire retardancy with the least amount of additive. The aim of a fire retardant is to reduce the likelihood of a fire by providing resistance to ignition and slowing the spread of flames. The LOI method is commonly employed to evaluate the fire retardancy of samples. Compounds with LOI values of 25 % or higher are considered self-extinguishing [40].

According to the LOI results summarized in Table 4, polyurethane exhibited a low oxygen index value similar to previously reported LOI values for conventional polyurethane [7,8]. In this study, the LOI

value of polyurethane was measured at 21.90 %. This value increased to 24.71 % upon the addition of 1 wt.% of compound **3a** to the coating formulation, and it rose further to 25.80 % with the incorporation of compound **3b**. These findings demonstrate that even a minimal amount of additives can enhance the LOI value of polyurethane. Moreover, the LOI value of compound **3a** was influenced by the length of the alkyl chain; a longer alkyl chain resulted in a higher LOI value. Previous research has indicated that cyclotriphosphazene with an alkyl chain enhanced thermal properties and fire retardancy owing to the synergistic fire-retardant effects of phosphorus and nitrogen [41,42]. The LOI results were also positively impacted by HCCP, which contains six chlorine atoms that contribute to its effective fire retardancy and thermal stability [43]. The presence of the Schiff base linking unit was found to enhance fire-retardant properties. This improvement can be attributed to the high thermal stability of the Schiff base molecules, which facilitates the formation of a char layer on the surface during the condensed phase [22]. All compounds demonstrated promising LOI results, suggesting their effectiveness as fire-retardant materials [17,18]. These results clearly indicate that addition of the HCCP-based compounds enhanced the LOI value of the pure polyurethane sample.

**Table 4.** Fire retardant properties of PU/HCCP compounds.

Compounds	LOI value (%)
Polyurethane, PU	21.90 (± 0.00)
PU/ <b>3a</b>	24.71 (± 0.00)
PU/ <b>3b</b>	25.80 (± 0.00)

## Physical Properties

### Determination of Resistance to Household Chemicals (ASTM D 1308-2)

After exposing the wood samples to eight different kinds of chemical household reagents for 24 hours at room temperature, it was observed that these had no effect on any of the HCCP-coated wood surfaces. These test results proved that PU lacquers offered good resistance to several household reagents.

However, PU lacquers have poor resistance to hot water above 79 °C. In this study, although the wood samples were exposed to hot distilled water and hot coffee at 100 °C, they did not contribute to discolouration or fracture of the film surface because the water temperature decreased as it was exposed to the cool air at room temperature. However, the soap, detergent and alkali solutions left slight stains on the surface of the PU wood panels. None of the other chemicals caused any blistering or erosion to the PU/**3a** and PU/**3b** coatings. According to Nejad *et al.*, (2013), among the household reagents tested, alkali solution had the most damaging effect on polyurethane. This might be due to the fact that the PU lacquer coating was not alkali-resistant [44].

### Determination of Temperature Change Resistance (ASTM D1211-97 (2001))

Significant physical factors impacting the durability of wooden panels include humidity, temperature extremes, and abrupt temperature changes. These conditions can lead to the degradation of protective coatings, causing problems such as loss of brightness, discolouration, cracking, and flaking. As a result, this degradation reduces both the lifespan and aesthetic value of wooden furniture and decorative products [2,45].

The temperature change test results are illustrated in Figure 7. As shown in the figure, the colour difference values ( $\Delta E^*$ ) for PU and HCCP/PU coated samples were distinguishable. Wood samples coated with the HCCP/PU showed decreasing values of  $\Delta E^*$ , while, the wood samples with PU showed a different behaviour:  $\Delta E^*$  increased from the first to the third cycle and then decreased in the fourth cycle. From the graph, the **3b**/PU coated sample had the highest  $\Delta E^*$  value. After four cycles of this test, HCCP/PU showed good resistance to dramatic temperature changes and maintained its original condition.

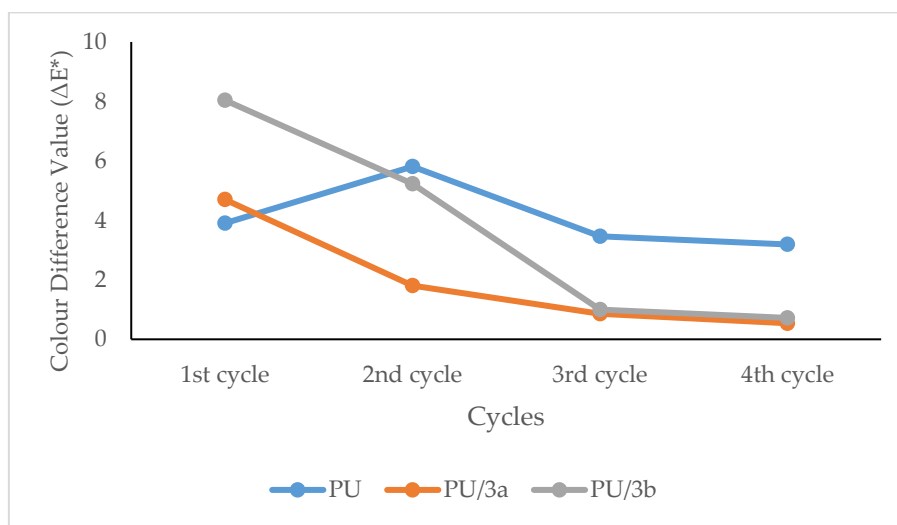


**Figure 7.** Colour reading test results for the temperature change resistance test.

**Table 5.** Classification of adhesion and impact of wood samples coated with different HCCP compounds.

Compound	Adhesion	Impact
Polyurethane, PU	0	4
PU/ <b>3a</b>	1	5
PU/ <b>3b</b>	1	5

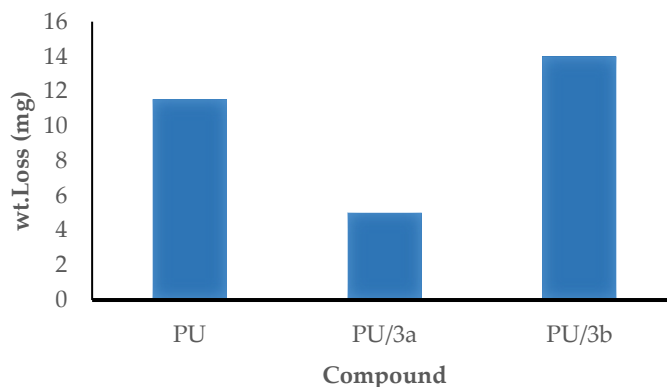


**Figure 8.** Weight loss of PU and PU/HCCP coatings after 100 abrasion cycles.

## Mechanical Properties

### *Cross-Cut Adhesion (ISO 2409-2007(E)) of HCCP/PU*

From Table 5, both the samples coated with PU/3a and PU/3b exhibited minor flaking of the coating at the intersections of the cuts. The affected cross-cut area was no greater than 5 % when a cross-cut blade with a width of 0.2 mm was used. In contrast, the edges of the cuts in the PU-coated sample remained completely smooth, with no squares of the lattice detaching.

These findings were in agreement with previous studies by El-Wahab *et al.*, (2020) [7] and El-Fattah *et al.*, (2017) [46]. They found that PU-coated samples had excellent adhesion properties. These results prove that polyurethane acts as a protective layer within the coating system and limits the cross-cut from going beyond the topcoat. However, HCCP-based compounds did not severely affect the adhesion characteristics of the overall polyurethane coating. Furthermore, the volatilization of solvents utilized in this experiment may lead to a reduction in adhesion. Consequently, if the coating is excessively thick, it could adversely affect its adhesion [47].

### *Impact (BS 3962 Part 6:1980) of HCCP/PU*

The effects of the ball impact on the wood surfaces are presented in Table 5, based on the specifications in BS 3962 Part 6:1980 Resistance to Mechanical Damage Impact. The specifications were described earlier in Table 2. The coating quality may be determined by evaluating the presence of a crack or defect on the surface area of the sample. The PU coated sample was categorized as 4, where a slight cracking (one circular crack around the edge of indentation) had occurred on the wood surface. This result was comparable with the findings of Erdinler *et al.* (2019). According to Erdinler *et al.* (2019), the thickness of the polyurethane coating was essential to protect the surface finish of the wood panel, while in this study, the addition of HCCP additives helped in protecting the surface finish [48]. The improved impact resistance of the coating systems was linked to the presence of

C-O-C and C-NH bonds [5]. In general, the elasticity of the lacquer determines the size and number of marks on the film caused by the fall of various objects, but it may also result in cracks in the film and even permanent indentations on the wood surface. Based on the data tabulated in Table 5, HCCP improved the impact resistance of the wood coating surface. Both the PU/3a and PU/3b samples did not show any cracking and thus were classified as 5.

### *Abrasion Resistance of HCCP/PU*

Generally, prolonged abrasive action leads to a reduction in film thickness and eventually to its total disappearance. Based on Figure 8, the weight loss of PU was 11.5 mg after 100 cycles of grinding. With the addition of HCCP, PU/3a had the best abrasion resistance. This outcome was attributed to the presence of C-O-C and C-NH bonds, and could also be due to the fact that in that range, the material was tough but also more resilient, as it could elongate and flex to avoid abrasion [5]. However, as seen in Figure 8, PU/3b seemed to exhibit poor abrasion resistance. The reason for this was that most of the PU/3b coating stayed on the wood surface and could not penetrate into its pores. The high weight loss of PU/3b was due to its uneven distribution during application.

## CONCLUSION

Tests on various wood coating systems revealed that the chemical composition of the HCCP derivatives used in the coatings significantly impacted its physical and mechanical properties. This study showed that household chemicals did not leave any stain on the finished surface of wood samples coated with HCCP additives after 24 hours. In the temperature change resistance test, HCCP/PU showed good resilience towards dramatic temperature changes. Based on these results, the HCCP additives improved the polyurethane coating. For the adhesion cross-cut test, both PU/3a and PU/3b had a rating of 1, while for the impact test, both were categorized as 5. For the abrasion test, PU/3a showed good abrasion

resistance compared to PU/3b and polyurethane. This may be attributed to the presence of C-O-C and C-NH bonds in the HCCP-based compounds. These specific chemical bonds and functional groups, including C-O-C and C-NH, influenced the impact resistance and abrasion properties of the wood coating systems.

#### ACKNOWLEDGEMENTS

The authors would like to acknowledge funding from Universiti Malaysia Sabah, Grant Number SPB0004-2020, and lab facility support from Universiti Sains Malaysia.

The authors declare that they have no conflicts of interest.

#### REFERENCES

1. Mali, P., Sonawane, N., Pawar, N. and Patil, V. (2022) UV-curing of novel tri-functional melamine-phosphate oligomer: An effect of coating with polyurethane acrylate toward mechanical, thermal, and flame retardant properties. *Polymers and Polymer Composites*, **30**, 1–23.
2. Živković, V., Turkulin, H. and Valdec, N. (2011) Surface of finished wood floorings - characteristics and testing, in: 22nd International Scientific Conference: Wood Is Good - EU Preaccession Challenges of the Sector, Proceedings, January, 201–211.
3. Evans, P. D., Haase, J. G., Seman, A. S. B. M. and Kiguchi, M. (2015) The search for durable exterior clear coatings for wood. *Coatings*, **5**, 830–864.
4. Jafarian, H., Demers, C. M. H., Blanchet, P. and Laundry, V. (2018) Effects of interior wood finishes on the lighting ambience and materiality of architectural spaces. *Indoor and Built Environment*, **27**, 786–804.
5. Pavlič, M., Petrič, M. and Žigon, J. (2021) Interactions of coating and wood flooring surface system properties. *Coatings*, **11**, 91.
6. Czeiszperger, R. and Duckett, E. J. (2019) Effective additives for improving abrasion resistance in polyurethane elastomers.
7. El-Wahab, H. A., El-Fattah, M. A., El-Alfy, H. M. Z., Owda, M. E., Lin, L. and Hamdy, I. (2020) Synthesis and characterisation of sulphonamide (Schiff base) ligand and its copper metal complex and their efficiency in polyurethane varnish as flame retardant and antimicrobial surface coating additives. *Progress in Organic Coatings*, **142**, 105577.
8. Ding, Y., Su, Y., Huang, J., Wang, T., Li, M. -Y. and Li, W. (2021) Flame retardancy behaviors of flexible polyurethane foam based on reactive dihydroxy P–N-containing flame retardants. *ACS Omega*, **6**, 16410–16418.
9. Mohd Sabee, M. M. S., Itam, Z., Beddu, S., Zahari, N. M., Mohd Kamal, N. L., Mohamad, D., Zulkepli, N. A., Shafiq, M. D. and Abdul Hamid, Z. A. (2022) Flame retardant coatings: Additives, binders, and fillers. *Polymers*, **14**, 2911.
10. Waldin, N. A. and Jamain, Z. (2023) Synthesis and mechanical property of hexasubstituted cyclotriphosphazene derivatives attached to hydrazine-bridge linkage with high fire retardancy. *Journal of Molecular Structure*, **1284**, 135330.
11. Usri, S. N. K., Jamain, Z. and Makmud, M. Z. H. (2021) A review on synthesis, structural, flame retardancy and dielectric properties of hexasubstituted cyclotriphosphazene. *Polymers*, **13**, 2916.
12. Sienkiewicz, A. and Czub, P. (2020) Flame retardancy of biobased composites—Research development. *Materials*, **13**, 5253.
13. Jiang, J., Li, J. and Gao, Q. (2015) Effect of flame retardant treatment on dimensional stability and thermal degradation of wood. *Construction and Building Materials*, **75**, 74–81.
14. Jamain, Z., Azman, A. N. A., Razali, N. A. and Makmud, M. Z. H. (2022) A Review on Mesophase and Physical Properties of Cyclotriphosphazene Derivatives with Schiff Base Linkage. *Crystals*, **12**, 1174.
15. Dagdag, O., Bachiri, A. E., Hamed, O., Haldhar, R., Verma, C., Ebenso, E. and Gouri, M. E. (2021) Dendrimeric Epoxy Resins Based on Hexachlorocyclotriphosphazene as a Reactive Flame Retardant Polymeric Materials: A Review. *Journal of Inorganic and Organometallic Polymers and Materials*, **31**, 3240–3261.
16. Jamain, Z., Khairuddean, M., Loh, M. L., Manaff, N. L. A. and Makmud, M. Z. H. (2020) Synthesis and characterization of hexasubstituted cyclotriphosphazene derivatives with azo linking unit. *Malaysian Journal of Chemistry*, **22**, 125–140.
17. Ma, T., Li, L., Wang, Q. and Guo, C. (2019) Construction of intumescent flame retardant and hydrophobic coating on wood substrates based on thiol-ene click chemistry without photoinitiators. *Composites Part B: Engineering*, **177**, 107357.
18. Huang, Y., Ma, T., Wang, Q. and Guo, C. (2019) Synthesis of biobased flame-retardant carboxylic

- acid curing agent and application in wood surface coating. *ACS Sustainable Chemistry & Engineering*, **7**, 14727–14738.
19. Usri, S. N. K., Jamain, Z. and Makmud, M. Z. H. (2022) Fire retardancy and dielectric strength of cyclotriphosphazene compounds with Schiff base and ester linking units attached to the electron-withdrawing side arm. *Polymers*, **14**, 4378.
  20. Cao, X., Yang, Y., Luo, H. and Cai, X. (2017) High efficiency intumescent flame retardancy between hexakis(4-nitrophenoxy) cyclotriphosphazene and ammonium polyphosphate on ABS. *Polymer Degradation and Stability*, **143**, 259–265.
  21. Fadeeva, V. P., Tikhova, V. D. and Nikulicheva, O. N. (2008) Elemental analysis of organic compounds with the use of automated CHNS analyzers. *Journal of Analytical Chemistry*, **63**, 1094–1106.
  22. Abd El-Wahab, H. (2015) Synthesis and characterisation of the flame retardant properties and corrosion resistance of Schiff's base compounds incorporated into organic coating. *Pigment & Resin Technology*, **44**, 101–108.
  23. Vidholdová, Z., Slabejová, G. and Šmidriaková, M. (2021) Quality of oil-and wax-based surface finishes on thermally modified oak wood. *Coatings*, **11**, 1–17.
  24. Mali, A. A. A. and Jamain, Z. (2023) Synthesis and characterization of non-mesogenic behavior of chalcone derivatives. *Malaysian Journal of Chemistry*, **25**, 158–168.
  25. Ha, S. T., Foo, K. L., Lin, H. C., Ito, M. M., Abe, K., Kunbo, K. and Sastry, S. S. (2012) Mesomorphic behavior of new benzothiazole liquid crystals having Schiff base linker and terminal methyl group. *Chinese Chemical Letters*, **23**, 761–764.
  26. Fadhil, M. Z. M., Mustamin, M. A. and Jamain, Z. (2024) Liquid crystalline behaviour of symmetrical thermotropic Schiff base compounds. *Journal of Molecular Structure*, **1315**, 138929.
  27. Jamain, Z., Khairuddean, M. and Saidin, S. A. (2019) Synthesis and characterisation of 1, 4-phenylenediamine derivatives containing hydroxyl and cyclotriphosphazene as terminal group. *Journal of Molecular Structure*, **1186**, 293–302.
  28. Rong, Y., Wentian, H., Liang, X., Yan, S. and Jinchun, L. (2015) Synthesis, mechanical and fire behaviours of rigid polyurethane foam with a reactive flame retardant containing phosphazene and phosphate. *Polymer Degradation and Stability*, **122**, 102–109.
  29. Taip, N. A. M., Jamain, Z. and Palle, I. (2022) Fire-retardant property of hexasubstituted cyclotriphosphazene derivatives with Schiff base linking unit applied as an additives in polyurethane coating for wood fabrication. *Polymers*, **14**, 3768.
  30. Demus, D., Goodby, J., Gray, G. W., Spiess, H. -W. and Vill, V. (1998) Handbook of Liquid Crystals, Low Molecular Weight Liquid Crystals I. Wiley-VCH: New York, NY, USA, Volume 2A.
  31. Frenkel, D. and Mulder, B. M. (2002) The hard ellipsoid-of-revolution fluid I. Monte Carlo simulations. *Molecular Physics*, **100**, 201–217.
  32. Jamain, Z. and Khairuddean, M. (2021) Synthesis and mesophase behaviour of benzylidene-based molecules containing two azomethine units. *Journal of Physics: Conference Series*, **1882**, 012120.
  33. Qu, T., Yang, N., Hou, J., Li, G., Yao, Y., Zhang, Q., He, L., Wu, D. and Qu, X. (2017) Flame retarding epoxy composites with poly(phosphazene: Co-bisphenol A)-coated boron nitride to improve thermal conductivity and thermal stability. *RSC Advances*, **7**, 6140–6151.
  34. Ma, H. -X., Li, J., Qiu, J. -J., Liu, Y. and Liu, C. -M. (2017) Renewable cardanol based star-shaped pre-polymer containing phosphazene core as potential bio-based green fire-retardant coatings. *ACS Sustainable Chemistry & Engineering*, **5**, 350–359.
  35. Huang, G., Huo, S., Xu, X., Chen, W., Jin, Y., Li, R., Song, P. and Wang, H. (2019) Realizing simultaneous improvements in mechanical strength, flame retardancy and smoke suppression of ABS nanocomposites from multifunctional graphene. *Composites Part B: Engineering*, **177**, 107377.
  36. Waldin, N. A. and Jamain, Z. (2023) The effect of alkyl terminal chain length of Schiff-based cyclotriphosphazene derivatives towards epoxy resins on flame retardancy and mechanical properties. *Polymers*, **15**, 1431.
  37. Sulaiman, N. I., Abu Bakar, M., Abu Bakar, N. H. H., Saito, N. and Thai, V. P. (2023) Modified sol–gel method for synthesis and structure characterization of ternary and quaternary ferrite-based oxides for thermogravimetrically carbon dioxide adsorption. *Chemical Papers*, **77**, 3051–3074.
  38. Lu, R., Wan, Y. -Y., Honda, T., Ishimura, T., Kamiya, Y. and Miyakoshi, T. (2006) Design and characterization of modified urethane lacquer coating. *Progress in Organic Coatings*, **57**, 215–222.

39. Wang, H., Du, X., Wang, S., Du, Z., Wang, H. and Cheng, X. (2020) Improving the flame retardancy of waterborne polyurethanes based on the synergistic effect of P–N flame retardants and a Schiff base. *RSC Advances*, **10**, 12078–12088.
40. Al-Shukri, S. M., Mahmood, A. T. and Hanbali, O. A. (2021) Spiro-cyclotriphosphazene with three functional end groups: Synthesis and structural characterization of new polycyclotriphosphazenes with Schiff-base groups. *Polimery/Polymers*, **66**, 341–349.
41. Levchik, G., Grigoriev, Y., Balabanovich, A., Levchik, S. and Klatt, M. (2000) Phosphorus–nitrogen containing fire retardants for poly (butylene terephthalate). *Polymer International*, **49**, 1095–1100.
42. Jamain, Z., Khairuddean, M., Kamaruddin, K. and Rui, Y. Z. (2021) Synthesis, structural elucidation and mesophase behaviour of hexasubstituted cyclotriphosphazene molecules with amide linking unit. *Malaysian Journal of Chemistry*, **23**, 213–222
43. Yang, R., Wang, B., Han, X., Ma, B. and Li, J. (2017) Synthesis and characterization of flame retardant rigid polyurethane foam based on a reactive flame retardant containing phosphazene and cyclophosphonate. *Polymer Degradation and Stability*, **144**, 62–69.
44. Nejad, M., Shafaghi, R., Ali, H. and Cooper, P. (2013) Coating performance on oil-heat treated wood for flooring. *BioResources*, **8**, 1881–1892.
45. Budakçı, M., Korkut, D. S. and Esen, R. (2010) The color changes on varnish layers after accelerated aging through the hot and cold-check test. *African Journal of Biotechnology*, **9**, 3595–3602.
46. El-Fattah, M. A., El-Wahab, H. A., Bashandy, M. S., El-Eisawy, R. A. and El-Hai, F. A. (2017) Potential application of some coumarin derivatives incorporated thiazole ring as ecofriendly anti-microbial, flame retardant and corrosion inhibitor additives for polyurethane coating. *Progress in Organic Coatings*, **111**, 57–66.
47. Liu, C. and Xu, W. (2022) Effect of coating process on properties of two-component waterborne polyurethane coatings for wood. *Coatings*, **12**, 1857.
48. Erdinler, E. S., Koc, K. H., Dilik, T. and Hazir, E. (2019) Layer thickness performances of coatings on MDF: polyurethane and cellulosic paints. *Maderas: Ciencia y Tecnologia*, **21**, 317–326.